

Scalable one-way quantum computer using on-chip resonator qubits

Chun-Wang Wu,* Ming Gao, Hong-Yi Li, Zhi-Jiao Deng, Hong-Yi Dai, Ping-Xing Chen, and Cheng-Zu Li
College of Science, National University of Defense Technology, Changsha 410073, People's Republic of China

(Received 11 November 2011; published 2 April 2012)

We propose a scalable and robust architecture for one-way quantum computation using coupled networks of superconducting transmission line resonators. In our protocol, quantum information is encoded into the long-lived photon states of the resonators, which have a much longer coherence time than the usual superconducting qubits. Each resonator contains a charge qubit used for the state initialization and the local projective measurement of the photonic qubit. Any pair of neighboring photonic qubits are coupled via a mediator charge qubit, and large photonic cluster states can be created by applying Stark-shifted Rabi pulses to these mediator qubits. The distinct advantage of our architecture is that it combines both the excellent scalability of the solid-state systems and the long coherence time of the photonic qubits. Furthermore, this architecture is very robust against the parameter variations.

DOI: [10.1103/PhysRevA.85.042301](https://doi.org/10.1103/PhysRevA.85.042301)

PACS number(s): 03.67.Lx, 03.67.Mn, 85.25.Cp

I. INTRODUCTION

Entanglement lies at the heart of quantum-information processing [1]. In 2001, Raussendorf and Briegel showed that a special type of highly entangled multiqubit states, called cluster states, can be used to implement one-way quantum computation [2]. In contrast to the standard quantum circuit model, which uses single- and two-qubit logic gates, a one-way quantum computer proceeds by a sequence of single-qubit measurements with classical feedforward of their outcomes. Moreover, this new kind of quantum computation is universal in the sense that any quantum circuit can be implemented on a suitable cluster state by single-qubit measurements only.

Quantum computation on cluster states has been studied in a variety of physical systems. To date, a small-scale one-way quantum computation has been demonstrated using linear optics techniques [3–5]. As quantum-information carriers, photonic qubits have the advantage of long coherence time. However, it is hard to construct a scalable optical one-way quantum computer due to the difficulty of large-scale integration in the linear optical devices. One-way quantum computation has also been explored in artificial solid-state systems (e.g., electron spins in quantum dots [6,7] and superconducting qubits [8–10]). Thanks to well-established microfabrication techniques, these solid-state qubits have very excellent scalability, but their inherent bad coherence properties remain a stumbling block. A physical architecture, which combines both the scalability and the long coherence time, is desirable for the realization of scalable one-way quantum computation.

Here, we propose an alternative architecture for one-way quantum computation using on-chip resonator qubits, which to some extent can overcome the two major roadblocks—decoherence and scalability—at the same time. In our protocol, quantum information is encoded into the zero- and one-photon states of the high- Q transmission line resonators. The good coherence properties of these photon states have been demonstrated in recent experiments. Many interesting

complex quantum states of photons, including the arbitrary superposition of Fock states [11] and NOON states with large particle numbers [12], have been synthesized in the laboratory. More recently, researchers have also proposed using these photon states to implement quantum computation based on the standard circuit model [13–15]. Each resonator in our architecture contains a charge qubit inside it, which is used for the state initialization and the local projective measurement of the photonic qubit. The controlled-phase interaction between neighboring photonic qubits can be implemented by applying 2π Stark-shifted Rabi pulses to the charge qubits at the resonator junctions, and large photonic cluster states can be created in $2d$ steps where d is the dimension of the resonator lattice. Moreover, our architecture is very robust against the parameter variations.

The paper is organized as follows. In Sec. II we describe our proposed architecture for one-way quantum computation in detail. In Sec. III, a concrete experimental procedure is presented including how to initialize the system, create the large photonic cluster states, and implement the local projective measurements of photonic qubits in the arbitrary basis. Finally, the experimental feasibilities are analyzed in Sec. IV.

II. PHYSICAL ARCHITECTURE

In principle, our idea is applicable for implementing one-way quantum computation based on an arbitrary dimensional resonator array. In Fig. 1, we only draw the one-dimensional (1D) linear resonator array and the two-dimensional (2D) resonator square lattice as simple examples.

For the 1D case, a linear array of n transmission line resonators, R_1, R_2, \dots, R_n , are connected via $n - 1$ superconducting charge qubits, $Q_1^2, Q_2^3, \dots, Q_{n-1}^n$ [Fig. 1(a)]. Any pair of neighboring resonators R_i and R_{i+1} ($1 \leq i \leq n - 1$) is required to have different resonance frequencies. Here, we assume that all the resonators R_p ($1 \leq p \leq n$, p is odd) have the same resonance frequency ω , while the other resonators R_q ($1 \leq q \leq n$, q is even) have the resonance frequency ω' ($\omega' \neq \omega$). Then the Hamiltonian that describes the photons in

*cwwu@nudt.edu.cn

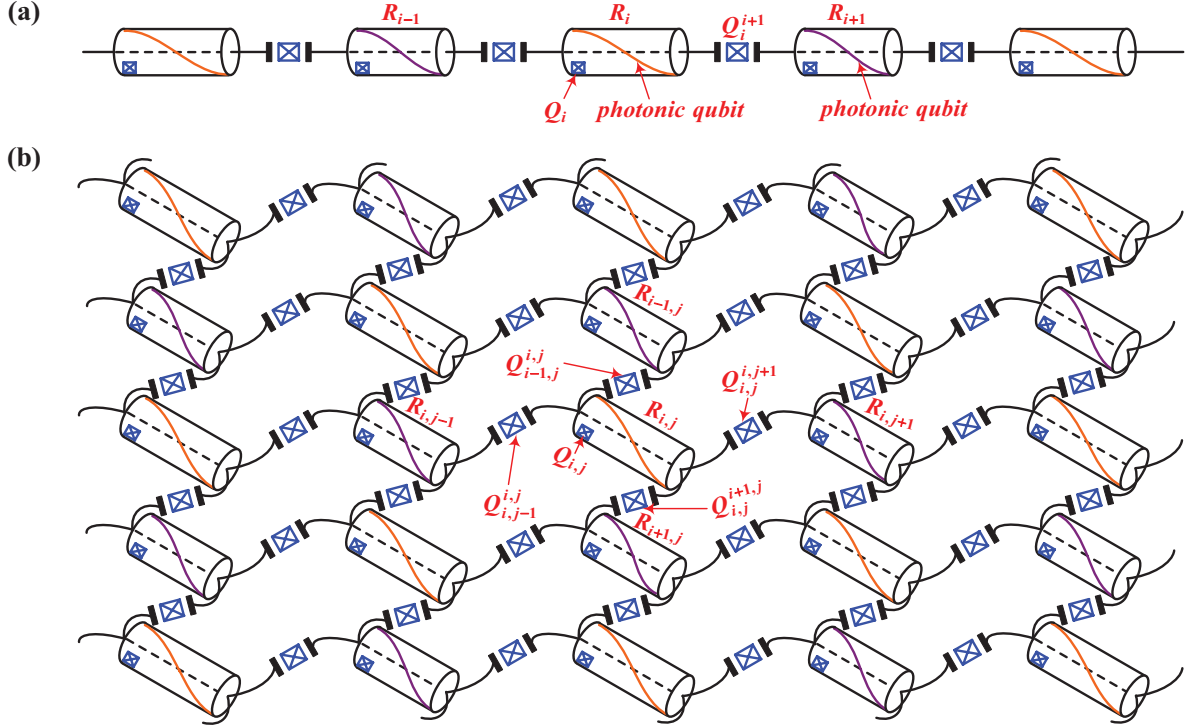


FIG. 1. (Color online) Schematic layout of our proposed architecture for one-way quantum computation based on the 1D linear resonator array (a) and the 2D resonator square lattice (b). Quantum information is encoded into the zero- and one-photon states of the high- Q microwave resonators. Each resonator contains a charge qubit used for the state initialization and the local projective measurement of the photonic qubit. Any pair of neighboring resonators have different resonance frequencies and are simultaneously capacitively coupled to a mediator charge qubit.

the resonator modes is (assuming $\hbar = 1$)

$$H_1^{1D} = \sum_{1 \leq p \leq n} \omega a_p^\dagger a_p + \sum_{1 \leq q \leq n} \omega' a_q^\dagger a_q, \quad (1)$$

where a_p^\dagger (a_q^\dagger) and a_p (a_q) are the photon creation and annihilation operators for resonator R_p (R_q). In our scheme, the photon number of any resonator at any time is engineered to be smaller than 2, and we use the zero-photon state $|0\rangle_i$ and one-photon state $|1\rangle_i$ of resonator R_i to represent the two states of logical qubit i . This kind of photonic qubit has a much longer coherence time than the usual superconducting qubits. Each resonator R_i contains a charge qubit Q_i used for the single-qubit rotations and readout of the photonic qubit i . Q_i 's role will be discussed in detail later. The neighboring resonators R_i and R_{i+1} are simultaneously capacitively coupled to a mediator charge qubit, Q_{i+1} . Let us denote the lowest two eigenstates of qubit Q_{i+1} with $|g\rangle_{i+1}$ and $|e\rangle_{i+1}$, which are separated by energy ϵ_{i+1} and coupled to its adjacent resonators with qubit-resonator coupling strength g . Then the Hamiltonian that describes the mediator qubits at the resonator junctions and their interaction with the resonators is

$$H_2^{1D} = \sum_{i=1}^{n-1} [\epsilon_{i+1} |e\rangle_{i+1} \langle e|_{i+1} + g(a_i^\dagger |g\rangle_{i+1} \langle e|_{i+1} + a_{i+1}^\dagger |g\rangle_{i+1} \langle e|_{i+1} + \text{H.c.})]. \quad (2)$$

We assume that control of Q_{i+1} can be exercised by a “shift” pulse to tune ϵ_{i+1} or a resonant microwave pulse to induce Rabi oscillation between $|g\rangle_{i+1}$ and $|e\rangle_{i+1}$.

For the 2D case, n^2 resonators $R_{i,j}$ ($1 \leq i, j \leq n$) are connected by $2n(n-1)$ charge qubits $Q_{i,j}^{i',j'}$ ($1 \leq i, j, i', j' \leq n$, $i' + j' - i - j = 1$) to form an $n \times n$ square lattice [Fig. 1(b)]. To suppress the photon hopping between neighboring resonators, we arrange that all the resonators $R_{p,q}$ ($1 \leq p, q \leq n$, $p+q$ is even) have the same resonance frequency ω , while the other resonators $R_{k,m}$ ($1 \leq k, m \leq n$, $k+m$ is odd) have the resonance frequency ω' . Then the Hamiltonian of the resonator modes reads

$$H_1^{2D} = \sum_{1 \leq p, q \leq n} \omega a_{p,q}^\dagger a_{p,q} + \sum_{1 \leq k, m \leq n} \omega' a_{k,m}^\dagger a_{k,m}, \quad (3)$$

where $a_{p,q}^\dagger$ ($a_{k,m}^\dagger$) and $a_{p,q}$ ($a_{k,m}$) are the photon creation and annihilation operators for resonator $R_{p,q}$ ($R_{k,m}$). Each resonator $R_{i,j}$ contains a charge qubit $Q_{i,j}$. The mediator qubit $Q_{i,j}^{i',j'}$'s lowest two eigenstates $|g\rangle_{i,j}^{i',j'}$ and $|e\rangle_{i,j}^{i',j'}$, separated by energy $\epsilon_{i,j}^{i',j'}$, are simultaneously capacitively coupled to $R_{i,j}$ and $R_{i',j'}$ with coupling strength g . Then the Hamiltonian that describes the mediator qubits at the resonator junctions and

their interaction with the resonators is

$$\begin{aligned}
 H_2^{2D} &= \sum_{1 \leq i, j \leq n} [\epsilon_{i,j}^{i,j+1} |e\rangle_{i,j}^{i,j+1} \langle e|_{i,j}^{i,j+1} + \epsilon_{i,j}^{i+1,j} |e\rangle_{i,j}^{i+1,j} \langle e|_{i,j}^{i+1,j} \\
 &+ g(a_{i,j}^\dagger |g\rangle_{i,j}^{i,j+1} \langle e|_{i,j}^{i,j+1} + a_{i,j+1}^\dagger |g\rangle_{i,j}^{i,j+1} \langle e|_{i,j}^{i,j+1} + \text{H.c.}) \\
 &+ g(a_{i,j}^\dagger |g\rangle_{i,j}^{i+1,j} \langle e|_{i,j}^{i+1,j} + a_{i+1,j}^\dagger |g\rangle_{i,j}^{i+1,j} \langle e|_{i,j}^{i+1,j} + \text{H.c.})],
 \end{aligned} \quad (4)$$

where $\epsilon_{i,n+1}^{i,n+1} = \epsilon_{n,j}^{n+1,j} = 0$ ($1 \leq i, j \leq n$) and $a_{i,n+1} = a_{n+1,j} = 0$ ($1 \leq i, j \leq n$).

In principle, the structures drawn in Fig. 1 can be extended to the higher dimensional case. In Ref. [16], the authors showed that it is possible to realize an effective arbitrary dimensional resonator lattice system by appropriately engineering the connections between the resonators fabricated on a 2D chip. However, with the increasing dimension, we must deal with the experimental problem of overlapping connections. Maybe it can be solved by fabricating crossing lines in different layers [17]. In fact, a 2D resonator square lattice suffices to implement the universal one-way quantum computation and overlapping connections are already needed for this case considering the necessary readout and control lines.

In our architecture, the coupling between any pair of adjacent resonators is independently tunable. By tuning the resonance frequency of a mediator charge qubit and making it far detuned from its neighboring resonators, the interaction between the two resonator qubits can be switched off. This is essential for the implementation of one-way quantum computation. First, once the photonic cluster states are generated, the interqubit coupling should be disabled to prevent the system state from further evolution. Second, an isolated photonic qubit is convenient for preparing the initial state and performing the local projective measurements.

Large cluster states can be generated by ‘‘fusing’’ the neighboring qubits via conditional phase gates [2]. In our architecture, the controlled-phase interaction between a pair of neighboring photonic qubits can be implemented by applying a 2π Stark-shifted Rabi pulse to the mediator charge qubit (Fig. 2). Now, we will explain this method based on the linear resonator array. We assume that the two involving resonators, R_i with resonance frequency ω and R_{i+1} with resonance frequency ω' , are isolated from the other resonators (by tuning the transition frequencies of Q_{i-1}^i and Q_{i+1}^{i+2} instantaneously to the far detuned regime), and their mediator charge qubit,

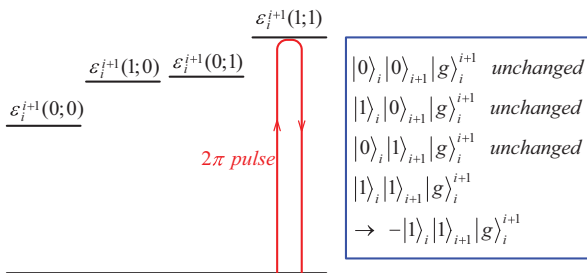


FIG. 2. (Color online) The conditional phase gate between a pair of neighboring photonic qubits can be implemented by applying a 2π Stark-shifted Rabi pulse to the mediator charge qubit.

Q_i^{i+1} , is operated in the strong dispersive regime. In this case, the qubit transition of Q_i^{i+1} can be resolved into separate spectral lines for different photon number states of R_i and R_{i+1} . Corresponding to n photons in R_i and n' photons in R_{i+1} , the Stark-shifted transition frequency of Q_i^{i+1} is [18]

$$\epsilon_i^{i+1}(n; n') = \epsilon_i^{i+1} + \frac{g^2}{\epsilon_i^{i+1} - \omega} (2n + 1) + \frac{g'^2}{\epsilon_i^{i+1} - \omega'} (2n' + 1). \quad (5)$$

An additional microwave field with frequency ω_d is applied to Q_i^{i+1} , which is described by

$$H_{\text{drive}} = \Omega(|e\rangle_i^{i+1} \langle g|_i^{i+1} e^{-i\omega_d t} + \text{H.c.}), \quad (6)$$

where Ω is the Rabi strength. Now we choose $\omega_d = \epsilon_i^{i+1}(1; 1)$ and $|\Omega| \ll \frac{2g^2}{|\epsilon_i^{i+1} - \omega|}, \frac{2g'^2}{|\epsilon_i^{i+1} - \omega'|}$, and then the mediator charge qubit Q_i^{i+1} undergoes Rabi oscillations if both R_i and R_{i+1} have one photon in them, but does nothing for other photon states. With the choice of $\Omega t = \pi$, the system state evolution is

$$\begin{aligned}
 |0\rangle_i |0\rangle_{i+1} |g\rangle_i^{i+1} &\rightarrow |0\rangle_i |0\rangle_{i+1} |g\rangle_i^{i+1}, \\
 |1\rangle_i |0\rangle_{i+1} |g\rangle_i^{i+1} &\rightarrow |1\rangle_i |0\rangle_{i+1} |g\rangle_i^{i+1}, \\
 |0\rangle_i |1\rangle_{i+1} |g\rangle_i^{i+1} &\rightarrow |0\rangle_i |1\rangle_{i+1} |g\rangle_i^{i+1}, \\
 |1\rangle_i |1\rangle_{i+1} |g\rangle_i^{i+1} &\rightarrow -|1\rangle_i |1\rangle_{i+1} |g\rangle_i^{i+1}.
 \end{aligned} \quad (7)$$

By tracing out the auxiliary system Q_i^{i+1} , we actually obtain a conditional phase gate between photonic qubits i and $i + 1$. The Stark-shifted Rabi oscillation used in this method has been experimentally demonstrated [19,20] and more recently was used in an entangled state synthesis algorithm [21].

Local operations of a photonic qubit can be performed with the help of a charge qubit injected into the resonator. High- Q resonator modes are advantageous for the quantum-information encoding but are adverse to the local measurements. To solve this problem, we can use the technique of engineering two modes of a resonator with different quality factors, which has been demonstrated experimentally in Ref. [22]. Now, we introduce the detailed configuration inside R_i . As shown in Fig. 3, the charge qubit Q_i , fabricated at one end of R_i , is capacitively coupled to the resonator modes. The transition between Q_i 's lowest two eigenstates $|g\rangle_i$ and $|e\rangle_i$, which are separated by energy ϵ_i , can be driven by applying a microwave pulse, U_i^d , to the gate. ϵ_i can be controlled using a local flux bias line by changing the applied magnetic flux Φ_i . The high- Q half-wave mode of R_i is used for encoding the quantum information, and R_i 's low- Q full-wave mode is strongly coupled to a measurement line fabricated at the resonator center. The state of Q_i can be measured by tuning ϵ_i close to the full-wave resonance frequency of R_i and applying a microwave field, U_i^m , at the input port of the measurement line [22].

III. ONE-WAY QUANTUM COMPUTATION USING ON-CHIP RESONATOR QUBITS

In this section, we give a concrete experimental procedure to implement one-way quantum computation based on our

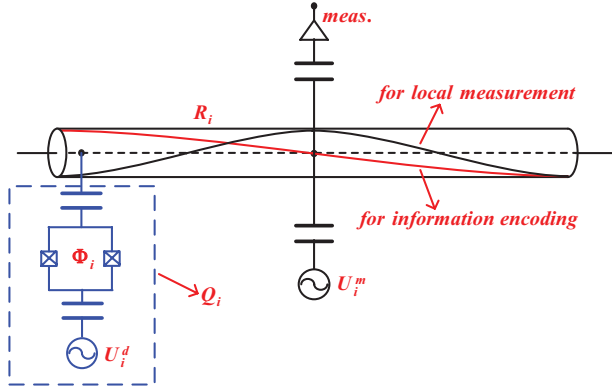


FIG. 3. (Color online) Detailed configuration inside R_i . The charge qubit Q_i is fabricated at one end of R_i and capacitively coupled to the resonator modes. The high- Q half-wave mode of R_i is used for the quantum-information encoding, while R_i 's low- Q full-wave mode is strongly coupled to a measurement line fabricated at the resonator center.

proposed architecture. We describe in detail the total manipulation process including state initialization, creation of the large photonic cluster states, and implementation of the local projective measurements in the arbitrary basis.

To generate the large photonic cluster states, the photonic qubits should be prepared in the state $\otimes_i \frac{1}{\sqrt{2}}(|0\rangle_i + |1\rangle_i)$. Initially, we assume the composite system of Q_i and R_i is in the ground state $|g\rangle_i|0\rangle_i$, and Q_i is detuned from R_i . Then, by applying a $\frac{\pi}{2}$ pulse to Q_i through the local driving line, the system state can be driven into $\frac{1}{\sqrt{2}}(|g\rangle_i - i|e\rangle_i)|0\rangle_i$. Next, we tune the transition frequency of Q_i to be resonant with R_i 's half-wave mode instantaneously. After time duration $t = \frac{3\pi}{2g_i}$, where g_i is the qubit-resonator coupling strength between Q_i and R_i , the system state evolves into $\frac{1}{\sqrt{2}}|g\rangle_i(|0\rangle_i + |1\rangle_i)$, and Q_i is tuned to be detuned from R_i again. Since each resonator has its own auxiliary charge qubit and driving line, parallel operation is allowed for this state initialization process.

For the 1D case, we show how to create the large photonic cluster state from the initial state $\otimes_{i=1}^n \frac{1}{\sqrt{2}}(|0\rangle_i + |1\rangle_i)$. In the first step, the photonic qubit pairs 1 and 2, 3 and 4, 5 and 6, \dots are isolated to form independent subsystems by tuning the transition frequencies of $Q_2^3, Q_4^5, Q_6^7, \dots$ to the far detuned regime instantaneously, and then we "fuse" the qubits 1 and 2, 3 and 4, 5 and 6, \dots using conditional phase gates by applying 2π Stark-shifted Rabi pulses to $Q_1^2, Q_3^4, Q_5^6, \dots$. After this step, the state of all the photonic qubits is

$$\frac{1}{2^{\frac{n}{2}}} \otimes_{i=1,3,5,\dots} (|0\rangle_i + \sigma_{i+1}^z |1\rangle_i)(|0\rangle_{i+1} + |1\rangle_{i+1}), \quad (8)$$

where σ_{i+1}^z is the Pauli-Z operator for qubit $i+1$. In the second step, we isolate photonic qubit pairs 2 and 3, 4 and 5, 6 and 7, \dots , and perform conditional phase gates for each pair as in the first step. Then we can prepare the n photonic qubits in the desired cluster state

$$\frac{1}{2^{\frac{n}{2}}} \otimes_{i=1}^n (|0\rangle_i + \sigma_{i+1}^z |1\rangle_i), \quad (9)$$

where $\sigma_{n+1}^z \equiv 1$.

In Ref. [23], Nielsen showed that 1D cluster states are not universal resource states because any one-way computation performed on 1D cluster states can efficiently be simulated on a classical computer. On the contrary, 2D cluster states have been proven to be universal resource states for one-way quantum computation in the sense that any quantum circuit can be implemented by performing a suitable sequence of single-qubit measurements on a sufficiently large 2D cluster state [24]. Therefore, creating large cluster states of dimensions higher than one is essential for implementing the universal quantum computation.

For the $n \times n$ resonator square lattice, the 2D photonic cluster state can be generated in four steps. First, we entangle the n qubits in each row into a 1D cluster state. Considering that this operation can be performed in parallel for different rows, it can be completed in two steps similar to the 1D case. After this operation, the state of all the photonic qubits is

$$\frac{1}{2^{\frac{n^2}{2}}} \otimes_{i=1}^n \left[\otimes_{j=1}^n (|0\rangle_{i,j} + \sigma_{i,j+1}^z |1\rangle_{i,j}) \right], \quad (10)$$

where $\sigma_{i,j+1}^z$ is the Pauli-Z operator for qubit $(i, j+1)$. Second, do the same for the n columns, then we can prepare the n^2 photonic qubits in the 2D cluster state

$$\frac{1}{2^{\frac{n^2}{2}}} \otimes_{i,j=1}^n (|0\rangle_{i,j} + \sigma_{i,j+1}^z \sigma_{i+1,j}^z |1\rangle_{i,j}), \quad (11)$$

where $\sigma_{i,n+1}^z \equiv \sigma_{n+1,j}^z \equiv 1$. Our procedure can be extended to the general case. For a general d -dimensional (d D) resonator cubic lattice, the d D cluster states can be generated in $2d$ steps.

In one-way quantum computation based on cluster states, calculations are carried out by a series of local measurements in the basis $B(\gamma) = \{|+\gamma\rangle, |-\gamma\rangle\}$, where $|\pm\gamma\rangle = (|0\rangle \pm e^{i\gamma}|1\rangle)/\sqrt{2}$ (γ is a real number). It is easy to verify that measuring a qubit in the basis $B(\gamma)$ is equivalent to performing a unitary rotation, U_γ , on the qubit followed by a measurement in the basis $\{|0\rangle, |1\rangle\}$, where $U_\gamma|+\gamma\rangle = |0\rangle$ and $U_\gamma|-\gamma\rangle = |1\rangle$. Now, using the experimental architecture shown in Fig. 3, we give a procedure for measuring the photonic qubit i in the basis $B(\gamma)$. Step 1, we let Q_i be resonant with R_i for time duration $t = \frac{\pi}{2g_i}$, and then the system state evolution is

$$(\alpha|0\rangle_i + \beta|1\rangle_i)|g\rangle_i \rightarrow (\alpha|g\rangle_i - i\beta|e\rangle_i)|0\rangle_i, \quad (12)$$

where $\alpha|0\rangle_i + \beta|1\rangle_i$ is the initial state of photonic qubit i . Single-qubit rotations of Q_i can be implemented by pulses of microwave applied to the gate driving line. Following the results of Ref. [18], different drive frequencies can be chosen to realize rotations around arbitrary axes in the x - z plane, and the rotation angle can be changed easily via varying the microwave pulse length. Let us define $R_\nu(\theta)$ ($\nu = x, y, z$) as the rotation of a qubit by an angle θ around the ν axis. Step 2, we rotate the charge qubit Q_i by an angle $\frac{\pi}{2}$ around the z axis and then the state of Q_i evolves into

$$R_z\left(\frac{\pi}{2}\right)(\alpha|g\rangle_i - i\beta|e\rangle_i) = \alpha|g\rangle_i + \beta|e\rangle_i. \quad (13)$$

After steps 1 and 2, the state of photonic qubit i is perfectly transferred to Q_i . Step 3, we first rotate the charge qubit Q_i by an angle $\frac{\pi}{2} - \gamma$ around the z axis and then by an angle $\frac{\pi}{2}$

around the x axis, in this way a single-qubit operation $U_\gamma^Q = R_x(\frac{\pi}{2})R_z(\frac{\pi}{2} - \gamma)$ is performed on Q_i which satisfies

$$\begin{aligned} U_\gamma^Q \left[\frac{1}{\sqrt{2}}(|g\rangle_i + e^{i\gamma}|e\rangle_i) \right] &= |g\rangle_i, \\ U_\gamma^Q \left[\frac{1}{\sqrt{2}}(|g\rangle_i - e^{i\gamma}|e\rangle_i) \right] &= |e\rangle_i. \end{aligned} \quad (14)$$

Step 4, tune the qubit transition frequency ϵ_i such that Q_i is decoupled from R_i 's half-wave mode but dispersively coupled to R_i 's full-wave mode. Then the state of Q_i can be measured in the basis $\{|g\rangle_i, |e\rangle_i\}$ by applying the microwave field U_i^m to the measurement line. With the help of Q_i , now we have completed the local measurement of photonic qubit i in the basis $B(\gamma)$ effectively.

IV. EXPERIMENTAL FEASIBILITY

In this section, we analyze the feasibility of our procedure by some rough calculations based on the practical experimental parameters. First, we give several necessary requirements our architecture parameters must meet. Note that the photon hopping between neighboring resonators will possibly make the relevant photonic qubits run outside of the $\{|0\rangle, |1\rangle\}$ manifold. To suppress this effect, the frequency difference $|\omega - \omega'|$ of the neighboring resonators must be much larger than the effective photon hopping rate κ_{hop} induced by the mediator charge qubit, i.e.,

$$|\omega - \omega'| \gg \kappa_{\text{hop}}. \quad (15)$$

The decoherences of the resonators and the charge qubits play significant roles in our procedure. The charge qubits situated in the resonators are used for state initialization and local measurements of the photonic qubits. Each mediator charge qubit participates in the one-way quantum computation process when ‘‘fusing’’ its neighboring resonator qubits using a conditional phase gate. To guarantee the high fidelity of the fusing process and the measurement process, the coherence time of the charge qubit τ_{cha} must be much longer than the required time of the conditional phase gate t_{cp} and the time of a local measurement t_{mea} , i.e.,

$$\tau_{\text{cha}} \gg t_{\text{cp}}, \quad \tau_{\text{cha}} \gg t_{\text{mea}}. \quad (16)$$

Finally, the resonators bear the quantum information for almost the total computation process; thus it is required that the photonic qubits have a coherence time, τ_{pho} , much longer than the required time of the total procedure, t_{tot} , i.e.,

$$\tau_{\text{pho}} \gg t_{\text{tot}}. \quad (17)$$

Now, we give a brief evaluation of the time scales involved. The qubit-resonator coupling strength up to $\frac{g}{2\pi} = 200$ MHz has been realized experimentally in Ref. [25]. In this case, the required time of a single-qubit rotation can be estimated as $t_{\text{sin}} \approx \frac{\pi}{g} = 2.5$ ns. Considering neighboring resonators R_i with $\frac{\omega}{2\pi} = 6.6$ GHz and R_{i+1} with $\frac{\omega'}{2\pi} = 7$ GHz and the mediator charge qubit Q_i^{i+1} with $\frac{\epsilon_i^{i+1}}{2\pi} = 8.6$ GHz, the effective photon hopping rate is approximately $\kappa_{\text{hop}} \approx \frac{g^2}{|\epsilon_i^{i+1} - \omega|} = 2\pi \times 20$ MHz, which is much smaller than the frequency

difference $|\omega - \omega'| = 2\pi \times 400$ MHz. When we implement the conditional phase gate between R_i and R_{i+1} , to sufficiently suppress the errors induced by the off-resonant transitions, the coupling strength of the Stark-shifted Rabi pulse Ω should satisfy $|\Omega| \ll \min(\frac{2g^2}{|\epsilon_i^{i+1} - \omega|}, \frac{2g^2}{|\epsilon_i^{i+1} - \omega'|}) = 2\pi \times 40$ MHz. Here, we choose $\Omega = 2\pi \times 4$ MHz; then the required time of the conditional phase gate is $t_{\text{cp}} = \frac{\pi}{\Omega} = 125$ ns. The low- Q full-wave resonator mode with photon decay rate $\kappa_{\text{pho}}^{\text{low}} = 2\pi \times 20$ MHz can be realized in the experiment by choosing big coupling capacitances for the measurement line [20]. Then the local projective measurement of Q_i in the basis $\{|g\rangle_i, |e\rangle_i\}$ can be implemented in a time scale of $t_{\text{mea}} \approx \frac{1}{\kappa_{\text{pho}}^{\text{low}}} = 8$ ns.

After each local measurement, the feedforward of the outcome must be performed to determine the next measurement basis. The measured signal has to travel to low-temperature electronics, undergo some sort of logic processing, and then travel back to the device. With several-meters-long connection cables, the propagation of the signal takes about 10 ns. Using high-speed electronic components, it is probable to complete the logic processing in tens of nanoseconds (e.g., in the proof-of-principle demonstration of the active feedforward technique for the linear optical system, the logic processing of the measured signal using electronics took about 7.5 ns [4]). Here, we assume that the total time for an individual feedforward step is $t_f = 30$ ns.

To implement one-way quantum computation based on a d D resonator cubic lattice consisting of N photonic qubits, we need the time of two single-qubit rotations for the state initialization, the time of $2d$ conditional phase gates for creating the cluster state, and the time of four single-qubit rotations followed by a local measurement and a feedforward step of the measurement outcome for measuring each photonic qubit; so the total time of the computation process t_{tot} is approximately

$$2dt_{\text{cp}} + N(4t_{\text{sin}} + t_{\text{mea}} + t_f) + 2t_{\text{sin}} = 250d + 48N + 5 \text{ (ns)}. \quad (18)$$

On the other hand, the charge qubit with coherence time $\tau_{\text{cha}} = 1 \mu\text{s}$ and the high- Q resonator mode with coherence time $\tau_{\text{pho}} = 5 \mu\text{s}$ are reasonable for the practical experimental setup [20]. Therefore, considering the necessary conditions [Eqs. (15)–(17)] and the practical experimental parameters, it is possible to perform one-way quantum computation based on a low-dimensional resonator lattice consisting of about ten resonator qubits.

Besides decoherence sources, another significant factor which prevents our one-way quantum computer from precise running is the imperfect local measurement. For the conventional measurement scheme discussed above, the fidelity of a single-shot local measurement is limited to typically 40%–60% by the amplifier noise. We can increase the measurement fidelity by replacing the conventional commercial amplifiers with specialized superconducting low-noise amplifiers [26], but at a cost of additional hardware complexity. In Ref. [27], the authors realized a high-fidelity measurement scheme which exploits the qubit-state-dependent bright-state onset power. Using this scheme, a single-shot measurement fidelity can be as high as 87%, and it does not require any change in the

conventional experimental setup. However, this measurement scheme takes a relatively long time (more than 100 ns for a single-shot measurement), which raises more stringent requirements on the system coherence. Compared with the decoherence sources, the imperfect local measurement affects our proposal in a more serious manner. For the case of $t_{\text{tot}} \ll \tau_{\text{pho}}$, the error induced by the decoherence of the photonic qubits can be approximated as $\frac{t_{\text{tot}}}{\tau_{\text{pho}}}$, which has a linear relation with N . However, the fidelity of the computation procedure will decrease exponentially with the number of the needed local measurements. If we perform one-way quantum computation of N photonic qubits, the error induced by the imperfect local measurements is about $1 - p^N$, where p is the fidelity of a single local measurement. Therefore, the precise running of our proposed one-way quantum computer still needs the optimization of the local measurements and the improved engineering of the coherence. In the near future, maybe we can use this architecture to create the large photonic cluster states.

Our procedure is very robust with regard to the device parameter variations, which are unavoidable in solid-state systems. Although we have assumed the same resonance

frequency for some resonators and the same qubit-resonator coupling strength in the preceding parts, these parameter homogeneities are not necessary in our procedure. Therefore, in the sample fabrication process, the requirements for homogeneity and reproducibility can be relaxed and met with current production technology.

In conclusion, we propose to construct a scalable one-way quantum computer using on-chip resonator qubits. The unique feature of our architecture is the combination of good scalability and long-lived qubits. With the recent progress in the multiresonator experiments [28], our proposal may serve as a guide to construct a small quantum computer consisting of more than a handful of qubits.

ACKNOWLEDGMENTS

This work was supported by the Foundation for the Author of National Excellent Doctoral Dissertation of China (Grant No. 200524), the Program for New Century Excellent Talents of China (Grant No. 06-0920), and the National Natural Science Foundation of China (Grants No. 11074307 and No. 11104353).

-
- [1] M. A. Nielsen and I. L. Chuang, *Quantum Computation and Quantum Information* (Cambridge University Press, Cambridge, UK, 2000).
 - [2] R. Raussendorf and H. J. Briegel, *Phys. Rev. Lett.* **86**, 5188 (2001); H. J. Briegel and R. Raussendorf, *ibid.* **86**, 910 (2001).
 - [3] P. Walther, K. J. Resch, T. Rudolph, E. Schenck, H. Weinfurter, V. Vedral, M. Aspelmeyer, and A. Zeilinger, *Nature (London)* **439**, 169 (2005).
 - [4] R. Prevedel, P. Walther, F. Tiefenbacher, P. Böhi, R. Kaltenbaek, T. Jennewein, and A. Zeilinger, *Nature (London)* **445**, 65 (2007).
 - [5] M. S. Tame, R. Prevedel, M. Paternostro, P. Böhi, M. S. Kim, and A. Zeilinger, *Phys. Rev. Lett.* **98**, 140501 (2007).
 - [6] M. Borhani and D. Loss, *Phys. Rev. A* **71**, 034308 (2005).
 - [7] A. Kolli, B. W. Lovett, S. C. Benjamin, and T. M. Stace, *Phys. Rev. Lett.* **97**, 250504 (2006).
 - [8] T. Tanamoto, Y. X. Liu, S. Fujita, X. Hu, and F. Nori, *Phys. Rev. Lett.* **97**, 230501 (2006).
 - [9] J. Q. You, X. B. Wang, T. Tanamoto, and F. Nori, *Phys. Rev. A* **75**, 052319 (2007).
 - [10] T. Tanamoto, Y. X. Liu, X. Hu, and F. Nori, *Phys. Rev. Lett.* **102**, 100501 (2009).
 - [11] M. Hofheinz *et al.*, *Nature (London)* **459**, 546 (2009).
 - [12] H. Wang *et al.*, *Phys. Rev. Lett.* **106**, 060401 (2011).
 - [13] A. Galiatdinov, A. N. Korotkov, and J. M. Martinis, e-print arXiv:1105.3997.
 - [14] A. Galiatdinov, e-print arXiv:1103.4641.
 - [15] F. W. Strauch, *Phys. Rev. A* **84**, 052313 (2011).
 - [16] D. I. Tsomokos, S. Ashhab, and F. Nori, *Phys. Rev. A* **82**, 052311 (2010).
 - [17] R. Harris *et al.*, *Phys. Rev. B* **82**, 024511 (2010).
 - [18] A. Blais, R. S. Huang, A. Wallraff, S. M. Girvin, and R. J. Schoelkopf, *Phys. Rev. A* **69**, 062320 (2004).
 - [19] D. I. Schuster *et al.*, *Nature (London)* **445**, 515 (2007).
 - [20] B. R. Johnson *et al.*, *Nat. Phys.* **6**, 663 (2010).
 - [21] F. W. Strauch, K. Jacobs, and R. W. Simmonds, *Phys. Rev. Lett.* **105**, 050501 (2010).
 - [22] P. J. Leek, M. Baur, J. M. Fink, R. Bianchetti, L. Steffen, S. Filipp, and A. Wallraff, *Phys. Rev. Lett.* **104**, 100504 (2010).
 - [23] M. A. Nielsen, *Rep. Math. Phys.* **57**, 147 (2006).
 - [24] M. Van den Nest, A. Miyake, W. Dür, and H. J. Briegel, *Phys. Rev. Lett.* **97**, 150504 (2006).
 - [25] L. Dicarlo, M. D. Reed, L. Sun, B. R. Johnson, J. M. Chow, J. M. Gambetta, L. Frunzio, S. M. Girvin, M. H. Devoret, and R. J. Schoelkopf, *Nature (London)* **467**, 574 (2010).
 - [26] L. Spietz, K. Irwin, and J. Aumentado, *Appl. Phys. Lett.* **95**, 092505 (2009).
 - [27] M. D. Reed, L. DiCarlo, B. R. Johnson, L. Sun, D. I. Schuster, L. Frunzio, and R. J. Schoelkopf, *Phys. Rev. Lett.* **105**, 173601 (2010).
 - [28] M. Mariantoni *et al.*, *Nat. Phys.* **7**, 287 (2011); H. Wang *et al.*, *Phys. Rev. Lett.* **106**, 060401 (2011).